ELSEVIER

Chemical Engineering Journal 66 (1997) 21–26

CHEMICAL ENGINEERING JOURNAL

Degassing effect and gas–liquid transfer in a high frequency sonochemical reactor

N. Gondrexon [a,1], V. Renaudin [a], P. Boldo [a], Y. Gonthier [a], A. Bernis [a], C. Petrier [b,*]

[a] *Laboratoire de Génie des Procédés, ESIGEC–Université de Savoie, 73376 Le Bourget du Lac, France*

[b] *Laboratoire de Chimie Moléculaire et Environnement ESIGEC–Université de Savoie, 73376 Le Bourget du Lac, France*

Received 29 August 1995; accepted 26 February 1996

Abstract

With a view to determining the parameters required to describe and to optimize sonochemical reactors, we have investigated gas–liquid transfer in a high frequency ultrasonic reactor. The effect of the sonicated volume and ultrasonic power on the dissolved dioxygen concentration in the reactor have been studied. Degassing action caused by cavitation bubbles and absorption caused by the acoustic fountain were shown. The study of the absorption phase leads to a model presented in this paper. The dissolved dioxygen concentration at equilibrium in the reactor which results from these two effects was shown to be constant in all cases.

Keywords: Degassing effect; Gas–liquid transfer; Sonochemical reactor; Ultrasonic reactor

1. Introduction

Ultrasonically induced cavitation is a way to promote heterogeneous or homogeneous chemical reaction [1]. The rate of sonochemical reactions is mainly determined by the physical and chemical properties of the solvant, such as the temperature, pressure and amount of dissolved gas [2,3].

The presence of dissolved gas reduces the cavitation threshold and it has been demonstrated that a flow of bubbling air has a marked effect on oxidative processes induced by ultrasound [4]. In relation to water treatment, several reports have described the ultrasonic degradation of toxic organic species [5–18]. We are especially interested in studying the sonochemical decomposition of aqueous phenolic solutions. It is now well known that, for such hydrophilic aromatic compounds with low vapor pressure, the main degradation pathway involves hydroxyl radicals [11–18], as a result of H_2O and O_2 sonolysis [19,20]. Moreover, the degradation rate under high frequency ultrasonic conditions has been shown to be higher than at low frequency [17].

The effect of dissolved dioxygen on the rate of the sonochemical degradation pathway is not yet fully understood, because of the ultrasound degassing action. Our interest in designing an appropriate reactor for sonochemistry leads us to investigate gas–liquid transfer in a homemade high frequency reactor. This paper describes the effects of several parameters, such as the volume of solution and acoustic power, on the degassing and regassing action when the upper liquid surface is exposed to the atmosphere. In addition, a reflector has been used to identify the role of the acoustic fountain and cavitation bubbles.

2. Experimental details

2.1. Experimental set-up

The experimental set-up is shown schematically in Fig. 1. The reactor consists of a PVC cylindrical body (1) (diameter, 100 mm; height, 100 mm) equipped with a stainless steel plate (2) at the bottom (diameter, 150 mm; thickness (equals half a wavelength), 5.84 mm). The high frequency ultrasound is produced by a 500 kHz piezoelectric transducer (3) (titanate–lead zirconate; diameter, 40 mm). This transducer (3) is attached to the stainless steel plate (2) and a homemade generator supplies this with an electrical output which varies from 0 to 100 W. The temperature in the reactor is kept constant by circulating cold water in a coil (4).

* Corresponding author.

[1] Present address: Laboratoire de Chimie des Eaux et Environnement ENSCR, 35700 Rennes, France.

PII S1385-8947(96)03124-7

Table 1
Absorption phase study: experimental data

V (ml)	P' (W)	P (W)	T (°C)	$C^*_{O_2}$ (mg l^{-1})	$C_{O_{2EQU}}$ (mg l^{-1})	τ (min)	$(K_La+B)\times10^4$ (s^{-1})	$K_La\times10^4$ (s^{-1})	$B\times10^4$ (s^{-1})
200	80	32	18	9.16	5.7	9.4	17.7	11	6.7
300	80	31	20.5	8.73	5.5	12	13.9	8.75	5.14
400	80	32	20.5	8.73	5.9	13.8	12.1	8.16	3.91
500	80	30	20.5	8.73	5.8	20	8.33	5.53	2.79
600	80	30	18	9.16	5.7	23.2	7.18	4.47	2.71
300	40	16	20.5	8.73	5.7	43	3.88	2.53	1.35
300	60	23	21	8.66	5.6	22.8	7.31	4.64	2.67
300	100	40	22	8.49	5.6	7	23.8	15.7	8.1

2.2. Measurement methods

2.2.1. Total ultrasonic power

The ultrasonic power dissipated in the liquid was estimated using the calorimetric method [21,22]. This calorimetric measurement of the ultrasonic power has shown that about 40% of the electrical output is transmitted to the solution (see Table 1).

2.2.2. Dissolved dioxygen concentration

The dissolved O_2 concentration was measured with the help of an 'oxymeter' (model Merck, 45T). Because this oxymeter cannot be placed directly in the sonochemical reactor to avoid electrical interference, a glass measuring cell has been developed and placed outside the reactor. A peristaltic pump (5) enables the circulation of the liquid (fresh water from an ion-exchange column) at a constant flow from the reactor to the cell (6) (loop volume, 10 ml; flow rate, 100 ml min^{-1}).

2.3. Experimental procedure

All the experiments were performed under atmospheric pressure and at constant temperature, but using two different set-ups. In the first set of experiments, the upper liquid surface was exposed to the atmosphere. However, in the second set of experiments, the upper air–liquid interface had been covered by a metal disk reflector (diameter, 98 mm; thickness, 5 mm) placed in the PVC body in contact with the upper liquid surface to avoid the formation of the acoustic fountain.

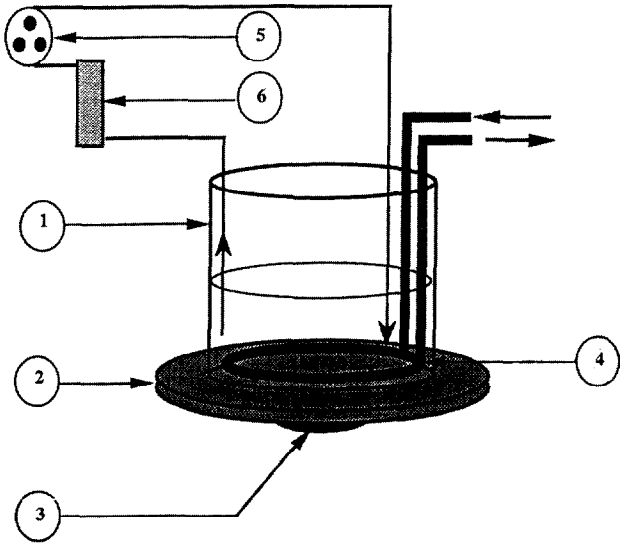

Fig. 1. Experimental set-up: 1, PVC body; 2, stainless steel plate; 3, piezoelectric transducer; 4, coil; 5, peristaltic pump; 6, dissolved dioxygen concentration measuring cell.

3. Experimental results

3.1. Preliminary observations

As shown in Fig. 2, when the upper liquid surface is exposed to the atmosphere, the dissolved O_2 concentration decreases and reaches a steady state soon after sonication begins. Sodium sulfide is then added to the medium to remove residual dissolved O_2. As soon as the sodium sulfide has reacted, O_2 absorption occurs. The dissolved O_2 concentration increases and reaches the same steady state. An 'equilibrium' concentration of dissolved O_2 can then be defined. This 'equilibrium' concentration of dissolved O_2 illustrates the degassing action of ultrasound and is less than the concentration of dissolved O_2 calculated at equilibrium under the same conditions of temperature and pressure in the absence of ultrasound (see Table 1). Under the same experimental conditions, if the upper air–liquid interface is covered with a

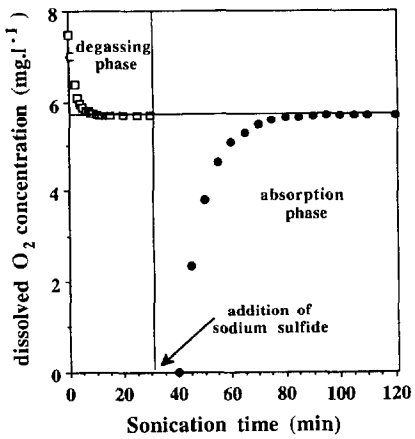

Fig. 2. Dissolved O_2 concentration as a function of the sonication time: volume, 200 ml; electrical output, 80 W; temperature, 18 °C.

reflector, then the degassing action appears to be more intense, as shown in Fig. 3. As soon as the reflector is removed, absorption occurs and the dissolved O_2 concentration reaches the same steady state as shown in Fig. 2.

According to these observations, the 'equilibrium' dissolved O_2 concentration defined in the case of a free air–liquid interface seems to result from the simultaneous contribution of two phenomena of transfer, as mentioned earlier by Henglein et al. [23]: liquid–gas transfer associated with the degassing action of the ultrasound, and a regassing action caused by the formation of the acoustic fountain at the free surface [24,25]. This acoustic fountain facilitates the uptake of gas from the atmosphere, with the degassing action being counterbalanced to a certain extent.

By using the reflector set-up, the acoustic fountain is removed and the degassing action cannot be counterbalanced. As shown in Fig. 4, increasing the ultrasonic power leads to an increased degassing rate. Therefore, it may be considered that the degassing action is the result of cavitation bubbles generated in the sonicated liquid, owing to the relationship between the number of cavitation bubbles and the ultrasonic power [26,27].

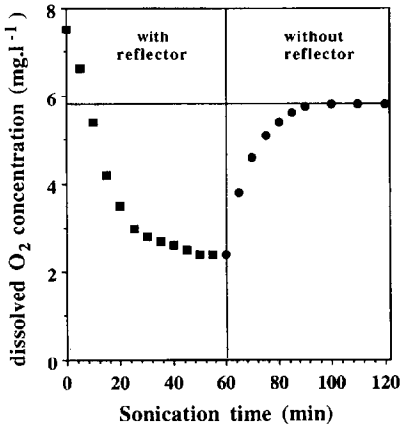

Fig. 3. Dissolved O_2 concentration as a function of the sonication time with and without a reflector: volume, 200 ml; electrical output, 80 W; temperature, 18 °C.

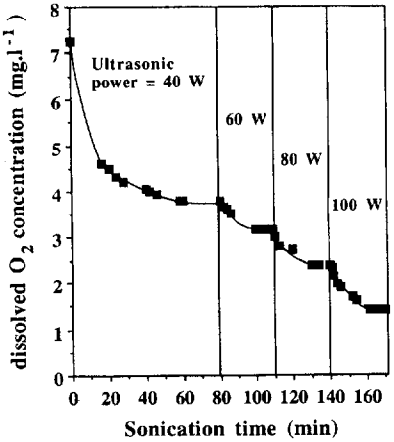

Fig. 4. Dissolved O_2 concentration as a function of the sonication time during the degassing phase with a reflector, showing the effect of the ultrasonic power: volume, 200 ml; temperature, 18 °C.

3.2. Study of the degassing phase

The effects of the ultrasonic power and the volume of solution on the degassing are presented in Figs. 5 and 6 respectively. The dissolved O_2 concentration decreases with increasing sonication time and reaches the same steady state in each case. This observation is consistent with the findings in previous work [23]. The sonication time required to reach the steady state is not affected by the ultrasonic power for a given volume of solution (see Fig. 5). As shown in Fig. 6, the liquid is degassed quicker when decreasing the sonicated volume for a given ultrasonic power. Although the ultrasonically induced degassing effect is widely used [28,29], no classical model of this phenomenon can be proposed and there is no report of the characterization of this phenomenon in the literature. Degassing under ultrasonic conditions appears as thermodynamically induced desorption in gas-oversaturated solutions [30].

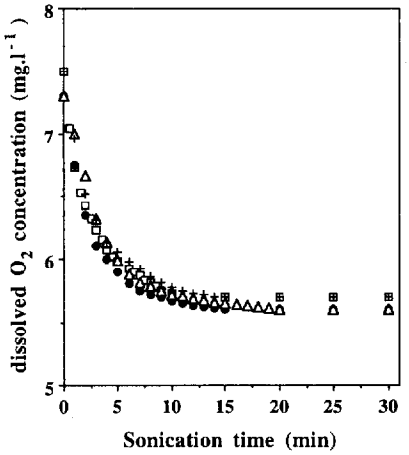

Fig. 5. Dissolved O_2 concentration as a function of the sonication time during the degassing phase, showing the effect of the ultrasonic power (electrical output): □, 40 W; ●, 60 W; △, 80 W; +, 100 W; sonicated volume, 300 ml.

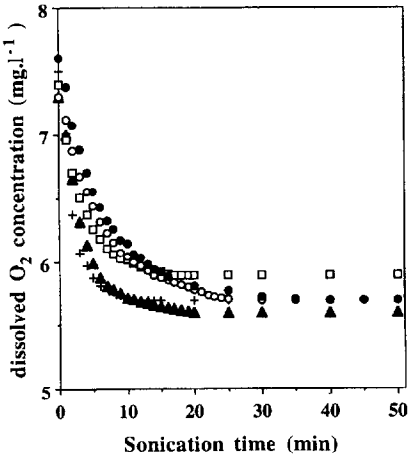

Fig. 6. Dissolved O_2 concentration as a function of the sonication time during the degassing phase, showing the effect of the sonicated volume: +, 200 ml; ▲, 300 ml; □, 400 ml; ○, 500 ml; ●, 600 ml; electrical output, 80 W.

3.3. Study of the absorption phase

In an alternative set-up, the effect of the ultrasonic power and the volume of solution on the dioxygen absorption have been investigated. The curves presented in Figs. 7 and 8 confirm the independence of the 'equilibrium' dissolved O_2 concentration versus the ultrasonic power and volume of sonicated solution. A link can also be established between the time required to reach the steady state and these two parameters: the greater the volume is or the lower the ultrasonic power is, the longer is the time required to reach the plateau.

3.3.1. Modelling

If cavitation bubbles are generated in the whole volume V of the reactor that is assumed to be well stirred, then the desorption flow is given by

BVC_{O_2}

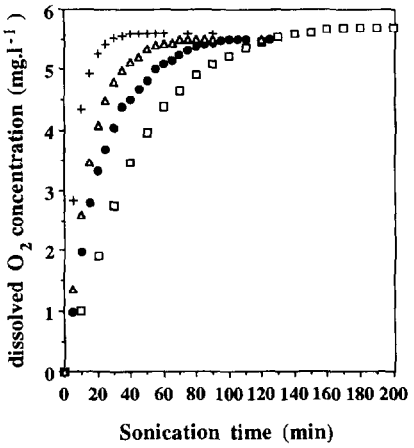

Fig. 7. Dissolved O_2 concentration as a function of the sonication time during the absorption phase, showing the effect of the ultrasonic power (electrical output): □, 40 W; ●, 60 W; △, 80 W; +, 100 W; sonicated volume, 300 ml.

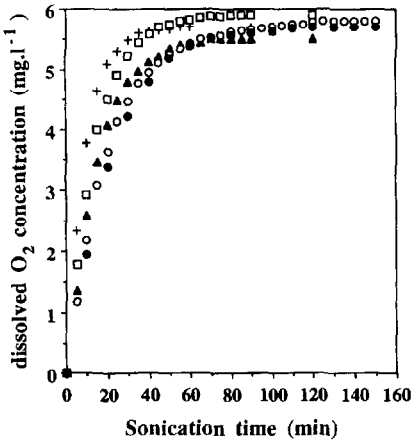

Fig. 8. Dissolved O_2 concentration as a function of the sonication time during the absorption phase, showing the effect of the sonicated volume: +, 200 ml; ▲, 300 ml; □, 400 ml; ○, 500 ml; ●, 600 ml; electrical output, 80 W.

in which B is a volumetric mass transfer coefficient and C_{O_2} is the dissolved dioxygen concentration in the reactor.

The absorption flow is given by

$$K_L\Omega(C^*_{O_2} - C_{O_2}) \quad \text{or} \quad K_LaV(C^*_{O_2} - C_{O_2})$$

in which a is the total liquid–air interface area (Ω) per unit volume of reactor, K_L is the mass transfer coefficient and $C^*_{O_2}$ is the dissolved dioxygen saturation concentration.

The dissolved dioxygen mass balance in the transient state in the reactor, which is assumed to be well stirred, is then

$$K_LaV(C^*_{O_2} - C_{O_2}) = BVC_{O_2} + V\frac{dC_{O_2}}{dt} \tag{1}$$

$$C_{O_2} + \frac{1}{K_La + B}\frac{dC_{O_2}}{dt} = \frac{K_La}{K_La + B}C^*_{O_2} \tag{2}$$

Here, we have

$$C_{O_2EQU} = \frac{K_La}{K_La + B}C^*_{O_2} \tag{3}$$

and

$$\tau = \frac{1}{K_La + B} \tag{4}$$

Eq. (2) becomes

$$C_{O_2} + \tau\frac{dC_{O_2}}{dt} = C_{O_2EQU} \tag{5}$$

Assuming that the dissolved O_2 concentration at the initial time is equal to 0 ($t = 0$ corresponds here to the beginning of the absorption phase), Eq. (5) can be solved as

$$C_{O_2} = C_{O_2EQU}\left[1 - \exp\left(-\frac{t}{\tau}\right)\right] \tag{6}$$

where the τ and C_{O_2EQU} values are determined from experimental curves. Eq. (6) is then used to calculate the dissolved O_2 concentration as a function of the sonication time during the absorption phase. A comparison between calculated and experimental data is reported in Fig. 9.

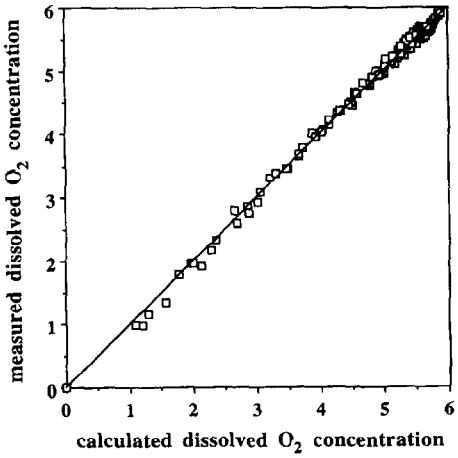

Fig. 9. Comparison between measured and estimated dissolved O_2 concentrations, with estimates based on Eq. (6).

3.3.2. Model parameters

The dissolved dioxygen saturation concentration $C^*_{O_2}$ is calculated according to the following equation obtained by correlation with common values of the saturated dissolved dioxygen concentration under atmospheric pressure:

$$C^*_{O_2} = \frac{461.5}{T(°C) + 32.3}$$

According to Eqs. (3) and (4), the coefficients K_La and B are respectively given by

$$K_La = \frac{C_{O_{2EQU}}}{\tau C^*_{O_2}}$$

and

$$B = \frac{1}{\tau} - K_La$$

Experimental results are reported in Table 1.

The volumetric mass transfer coefficients K_La and B can be estimated from

$$K_La = 2.9 \times 10^{-10}\frac{P^2}{V} \quad \text{or} \quad K_L\Omega = 2.9 \times 10^{-10}P^2 \qquad (7)$$

and

$$B = 1.55 \times 10^{-10}\frac{P^2}{V} \qquad (8)$$

in which P is the total ultrasonic power (W) determined by calorimetry and V is the sonicated volume (m^3). Fig. 10 shows a comparison between experimental and estimated data.

3.3.3. Discussion

The coefficient B, taken here to be a volumetric mass transfer coefficient, increases on increasing the ultrasonic power for a given volume. When the total acoustic power is kept constant, B decreases with increasing sonicated volume. Because the degassing action results from the cavitation bubbles generated in the sonicated liquid, the relationship between the number of cavitation bubbles and the ultrasonic power [26,27] has to be considered and extended to the volumetric ultrasonic power notion to explain these two points.

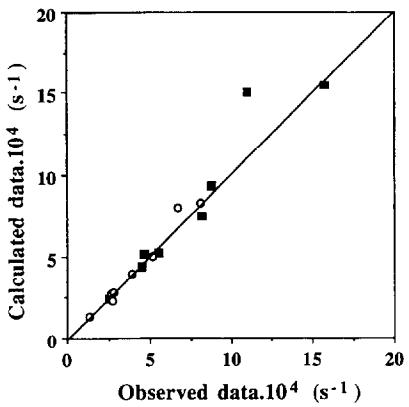

Fig. 10. Comparison between observed and estimated data, with estimates based on Eqs. (7) and (8): ■, K_La; ○, B.

The absorption phenomenon operates through the air–liquid interface. This free plane interface without ultrasound is disturbed as soon as sonication begins. The acoustic radiation pressure on the liquid–air interface causes the appearance of an acoustic fountain [24,25] shaped like a cone with diameter d and height h. As mentioned earlier by Bogodorovskii and Romanov [25], the linear dependence of the height h of the relief on the ultrasonic power has been shown experimentally, while the diameter d remains unchanged. Thus, increasing the ultrasonic power leads to an increased total exchange surface. Moreover, acoustically induced convective patterns which arise in the reactor are more intense when the ultrasonic power is increased for a given volume, as observed by Cadwell and Fogler [27]. These two effects result in an increased K_La coefficient with increasing ultrasonic power for the same sonicated volume. The increase in the volumetric mass transfer coefficient may be explained in terms of the increase in the exchange surface and increase in the rate of surface renewal.

When the ultrasonic power is kept constant, the height h of the acoustic fountain is constant, regardless of the liquid height in the reactor. This will not change the total exchange surface. Therefore, the parameter a that is defined as the total exchange surface (Ω) per unit volume of reactor decreases when increasing the volume. Moreover, convective patterns decreases in intensity with greater solution volumes. An increase in teh sonicated volume consequently leads to a decrease in the K_La coefficient.

From the data reported in Table 1, it can be seen that the ratio B/K_La is constant, i.e.

$$\frac{B}{K_La} = 0.55 \pm 0.08$$

By substitution in Eq. (3), this leads to

$$C_{O_{2EQU}} = (0.64 \pm 0.04)C^*_{O_2}$$

The 'equilibrium' dissolved dioxygen concentration $C_{O_{2EQU}}$ seems to depend only on the saturation concentration of dissolved dioxygen $C^*_{O_2}$. The effect of other parameters, such as the temperature or pressure, has now to be investigated to confirm this result.

4. Conclusions

In this paper, characteristics of high frequency ultrasound degassing effects have been considered. The dissolved O_2 concentration reaches a steady state soon after sonication begins. The 'equilibrium' dissolved O_2 seems to result from the superposition of two simultaneous mechanisms: a degassing action that results from cavitation bubbles, and an absorption phenomenon that involves the acoustic fountain effect. However, the independence of the 'equilibrium' dis-

solved O_2 concentration from the sonicated volume and ultrasonic power was not expected.

Such observations are of importance in the design of appropriate reactors for sonochemistry and are a matter which should concern different processes based on ultrasonic technology.

Appendix A. Nomenclature

a	total exchange surface per unit volume of reactor ($m^2\ m^{-3}$)
B	degassing volumetric mass transfer coefficient(s^{-1})
C_{O_2}	dissolved dioxygen concentration in the reactor ($mg\ l^{-1}$)
$C^*_{O_2}$	dissolved dioxygen saturation concentration ($mg\ l^{-1}$)
C_{O2EQU}	'equilibrium' dissolved dioxygen concentration ($mg\ l^{-1}$)
K_L	mass transfer coefficient ($m\ s^{-1}$)
P'	electrical output (W)
P	ultrasonic power estimated by calorimetry (W)
t	sonication time (s)
T	temperature of sonicated solution (°C)
V	volume of reactor (m^3)
Ω	total exchange surface (m^2)
τ	time constant (s)

References

[1] A. Henglein, *Ultrasonics, 25* (1987) 6–16.

[2] A.A. Atchley and L.A. Crum, in K.S. Suslick (ed.), *Ultrasound—Its Chemical, Physical and Biological Effects*, VCH, New York, 1988, p. 1.

[3] T.J. Mason, *Practical Sonochemistry: User's Guide to Applications in Chemistry and Chemical Engineering*, Ellis Horwood, 1991, chapter 1.

[4] C.M. Sehgal and S.Y. Wang, *J. Am. Chem. Soc., 103* (1981) 6606–6011.

[5] J.W. Chen, J.A. Chang and G.V. Smith, *Chem. Eng. Prog. Symp. Ser., 67* (1971) 18–26.

[6] H.M. Cheung, A. Bhatnagar and G. Jansen, *Env. Sci. Technol., 25* (1991) 1510–1512.

[7] J.M. Wu, H.S. Huang and C.D. Livengoo, *Env. Prog., 11* (1992) 195–202.

[8] K. Inaztu, Y. Nagata and Y. Maeda, *Chem. Lett.*, (1993) 57–60.

[9] A. Kotronarou, G. Mills and M.R. Hoffmann, *Env. Sci. Technol., 26* (1992) 1460–1462.

[10] A. Kotronarou, G. Mills and M.R. Hoffmann, *Env. Sci. Technol., 26* (1992) 2420–2428.

[11] N. Serpone, R. Terzian, P. Colarusso, C. Minero, E. Pelizzetti and H. Hidaka, *Res. Chem. Intermed., 18* (1992) 183–202.

[12] S. Okouchi, O. Nojima and T. Arai, *Water Sci. Technol., 26* (1992) 2053–2056.

[13] C. Petrier, M. Micolle, G. Merlin, J.L. Luche and G. Reverdy, *Env. Sci. Technol., 26* (1992) 1639–1642.

[14] A. Kotronarou, G. Mills and M.R. Hoffmann, *J. Phys. Chem., 95* (1991) 3630–3638.

[15] M. Cost, G. Mills, P. Glisson and J. Lakin, *Chemosphere, 27* (1993) 1737–1743.

[16] J. Berlan, F. Trabelsi, H. Delmas, A.M. Wilhem and J.F. Pretrignani, *Ultrason. Sonochem., 1* (1994) S97–S102.

[17] C. Petrier, M.F. Lamy, A. Francony, A. Benahcene, B. David, V. Renaudin and N. Gondrexon, *J. Phys. Chem., 98* (1994) 10514–10520.

[18] N. Serpone, R. Terzian, H. Hidaka and E. Pelizzetti. *J. Phys. Chem, 98* (1994) 2634–2640.

[19] P. Riesz, D. Berdahl and C.L. Christman, *Env. Health Perspect., 64* (1985) 233–252.

[20] C.H. Fischer, E.J. Hart and A. Henglein, *J. Phys. Chem., 90* (1986) 1954.

[21] V. Renaudin, N. Gondrexon, P. Boldo, C. Petrier, Y. Gontier and A. Bernis, *Ultrason. Sonochem., 1* (1994) S81–S85.

[22] M. Gutierrez and A. Henglein, *J. Phys. Chem., 94* (1990) 3625–3628.

[23] A. Henglein, D. Herburger and M. Gutierrez, *J. Phys. Chem., 96* (1992) 1126–1130.

[24] R.M.G. Boucher, *Br. Chem. Eng., 15* (1970) 363–367.

[25] V.V. Bogodorodskii and V.N. Romanov, *Sov. Phys. Acous., 8* (1963) 326–329.

[26] P.K. Chendke and H.S. Fogler, *Chem. Eng. J., 8* (1974) 165–178.

[27] M.L. Cadwell and H.S. Fogler, *Chem. Eng. Prog. Symp. Ser., 67* (1971) 124–127.

[28] K.S. Suslick, *Ultrasound—Its Chemical, Physical and Biological Effects*, VCH, New York, 1988, chapter 3, pp. 110–111.

[29] T.J. Mason, *Ultrasonics, 30* (1992) 192–196.

[30] G. Wild and N. Midoux, *Houille Blanche, 2* (1988) 163–171.